

AD-A096 408

MASSACHUSETTS INST OF TECH CAMBRIDGE

F/6 7/3

REDUCTIVE ELIMINATION OF H-H, H-CH₃, AND CH₃-CH₃ FROM BIS(PHOSPHO-ETC(U))

N00014-75-C-0970.

UNCLASSIFIED

TR-14

NL

1 OF 1
404
09606

END
DATE
4-8-1
DTIC

AD A 096408

LEVEL II

12

UNCLASSIFIED
SECURITY CLASSIFICATION OF THIS PAGE (When Data Entered)

REPORT DOCUMENTATION PAGE		READ INSTRUCTIONS BEFORE COMPLETING FORM
1. REPORT NUMBER 14.	2. GOVT ACCESSION NO. AD-A096	3. RECIPIENT'S CATALOG NUMBER 408
4. TITLE (and Subtitle) Reductive Elimination of H-H, H-CH ₃ , and CH ₃ -CH ₃ from Bis(phosphine)platinum(II), -palladium(II), and -nickel(II) Complexes: A Theoretical Study Using the SCF-X _α -SW Method.		5. TYPE OF REPORT & PERIOD COVERED Interim
7. AUTHOR(s) Anna C. Balazs, Keith H. Johnson, and George M. Whitesides		6. PERFORMING ORG. REPORT NUMBER N00014-75-C-0970
9. PERFORMING ORGANIZATION NAME AND ADDRESS Departments of Materials Science and Engineering and Chemistry, M.I.T., Cambridge, MA 02139		10. PROGRAM ELEMENT, PROJECT, TASK AREA & WORK UNIT NUMBERS Task No. NR056-596
11. CONTROLLING OFFICE NAME AND ADDRESS Office of Naval Research Department of the Navy Arlington, Virginia 22217		12. REPORT DATE March 4, 1981
14. MONITORING AGENCY NAME & ADDRESS (if different from Controlling Office)		13. NUMBER OF PAGES 15. SECURITY CLASS. (of this report) Unclassified
16. DISTRIBUTION STATEMENT (of this Report) Approval for public release; distribution unlimited.		15a. DECLASSIFICATION/DOWNGRADING SCHEDULE
17. DISTRIBUTION STATEMENT (of the abstract entered in Block 20, if different from Report)		MAR 17 1981 DTIC ELECTRONIC REPRODUCTION
18. SUPPLEMENTARY NOTES		
19. KEY WORDS (Continue on reverse side if necessary and identify by block number) reductive elimination; SCF-X _α -SW method		
20. ABSTRACT (Continue on reverse side if necessary and identify by block number) Self-consistent-field X _α scattered-wave (SCF-X _α -SW) calculations have been carried out for two series of organometallic complexes (L = H ₃ P: L ₂ PtH ₂ , L ₂ Pt(H)CH ₃ , and L ₂ Pt(CH ₃) ₂ ; L ₂ Ni(CH ₃) ₂ , L ₂ Pd(CH ₃) ₂ , and L ₂ Pt(CH ₃) ₂). These calculations suggest a correlation between the relative rates of reductive elimination (L ₂ MXY → L ₂ M + XY) and the molecular orbital character of the starting complexes: those compounds which eliminate XY relatively rapidly have occupied molecular orbitals with pronounced M-X(Y) antibonding character.		

~~UNCLASSIFIED~~

SECURITY CLASSIFICATION OF THIS PAGE (When Data Entered)

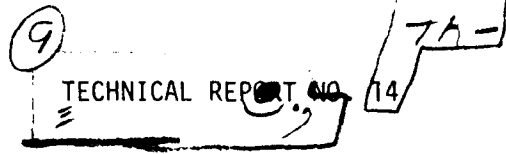
those which eliminate XY slowly have only vacant M-X(Y) antibonding orbitals. No single orbital (HOMO or other) dominates the M-X(Y) bonding in these complexes: bonding and antibonding character is distributed among several of the valence orbitals. We propose a simple model to correlate the occupancy of antibonding M-X(Y) orbitals and rates of reductive elimination with the relative electronegativities of M and X(Y). The limitations of this model, and alternates to it, are described briefly.

~~UNCLASSIFIED~~

OFFICE OF NAVAL RESEARCH

Contract N00014-75-C-0970

Task No. NR 056-596



Reductive Elimination of H-H, H-CH₃, and
CH₃-CH₃ from Bis(phosphine)platinum(II), -palladium(II), and
-nickel(II) Complexes: A Theoretical Study Using the SCF-X_α-SW Method.

by

⑫ Anna C. Balazs, Keith H. Johnson, and George M. Whitesides

Department of Materials Science and Engineering

and

*Department of Chemistry

Massachusetts Institute of Technology

Cambridge, Massachusetts 02139

⑪ 4 Mar 81

⑫ 42

March 4, 1981

Reproduction in whole or in part is permitted for
any purpose of the United States Government

Approved for Public Release: Distribution Unlimited

2240000

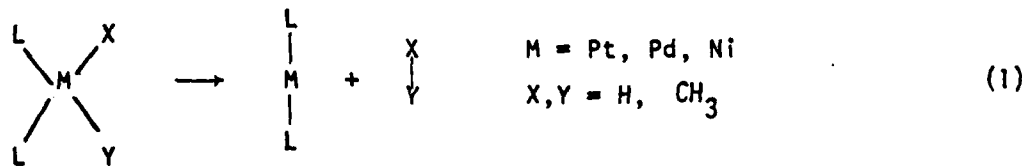
11

81316038

Accession For	
NTIS GRAIL	
DTIC TAB	
Unannounced	
Justification	
By	
Approved by	
Available to	
Printed by	
A	

Introduction

This paper outlines a theoretical study of the electronic structure of several transition metal organometallic compounds having the structure $(H_3P)_2MXY$ ($X, Y = H, CH_3$) carried out using the self-consistent-field-X α scattered wave (SCF-X α -SW) method. It examines the characteristics of the upper occupied molecular orbitals of these complexes, and looks for correlations between these characteristics and the relative rates of reductive elimination of the elements of XY from them (eq. 1, $L = PH_3$). These reactions, and the reactions



which are their microscopic reverse, are models for the individual steps in a number of useful processes catalyzed by transition metals (homogeneous hydrogenation, coupling, and reduction; perhaps heterogeneous hydrogenation and dehydrogenation.)¹

The calculations described here were stimulated by two qualitative generalizations which are emerging from current experimental work in the organometallic chemistry of the d^8 metals. First, the rates of the reductive elimination reactions of the type represented by eq. 1 appear to decrease in the order $k_{L_2MH_2} > k_{L_2M(H)CH_3} > k_{L_2M(CH_3)_2}$ for a series in which the metal and its ligands L are constant. Second, the rates of these reactions

seem to increase in the order $k_{L_2Pt(CH_3)_2} < k_{L_2Pd(CH_3)_2} < k_{L_2Ni(CH_3)_2}$ in a series in which only the metal changes.²⁻⁴ Unfortunately, there are presently few strictly comparable examples in either series, and the value of these generalizations remains to be established. Further, we must assume that those reductive eliminations which are known follow the same mechanism and are concerted in order to compare their rates.⁵ These assumptions are probably correct for many cases, but convincing experimental evidence supporting their correctness exists in only a few.^{2-4,6} Their uncertain generality notwithstanding, these two series serve as a starting point for theoretical consideration of this type of chemistry.

At the outset, we acknowledge that this work is directed to only one of several factors which might in principle influence the relative rates in these series: viz., the electronic structure of the L_2MXY group. Entropic effects (which are probably similar for all the reactions subsumed by eq 1⁷) and nonbonded steric effects (which may be significantly different for different of these reactions⁸) are neglected entirely. We touch only briefly on differences in the energies of the assumed products (L_2M , X-Y), and make no estimates of energies of transition states. Limitations intrinsic to the version of the SCF-Xa-SW method used here further constrain the types of questions concerning local electronic structure which can be addressed (see below). The objective of the work is thus not to discuss which features of the electronic structure of the metal and its directly bonded ligands determine the relative rates of eq 1, or even to try to establish whether this electronic structure does in fact dominate these rates. Addressing either question would require the ability to construct potential surfaces (including enthalpic contributions due to nonbonded interactions and entropic terms) describing the decompositions in a detail which is presently beyond

the capability of this (and other) theoretical methods. Instead, the objective of this work is to explore the limited question of whether the trends in rates correlate with physically interpretable characteristics of the local electronic structure of the reactants, L_2MXY . If such correlations exist and can be identified, they may be useful in guiding the synthesis of mechanistically or synthetically useful organometallic complexes. Any more sophisticated effort to distinguish between "correlation" and "cause" in this area of organometallic chemistry must be postponed until more and better experimental data (especially data establishing the structures of typical transition states) and more accurate theoretical methods are available.

Previous theoretical discussions of rates of reductive elimination reactions include works by Hoffmann, et al.⁹, Brateman and Cross¹⁰, and Åkermark¹¹. Additional relevant calculations have been described by Goddard, Anderson, and others¹².

Methods

~~~~~

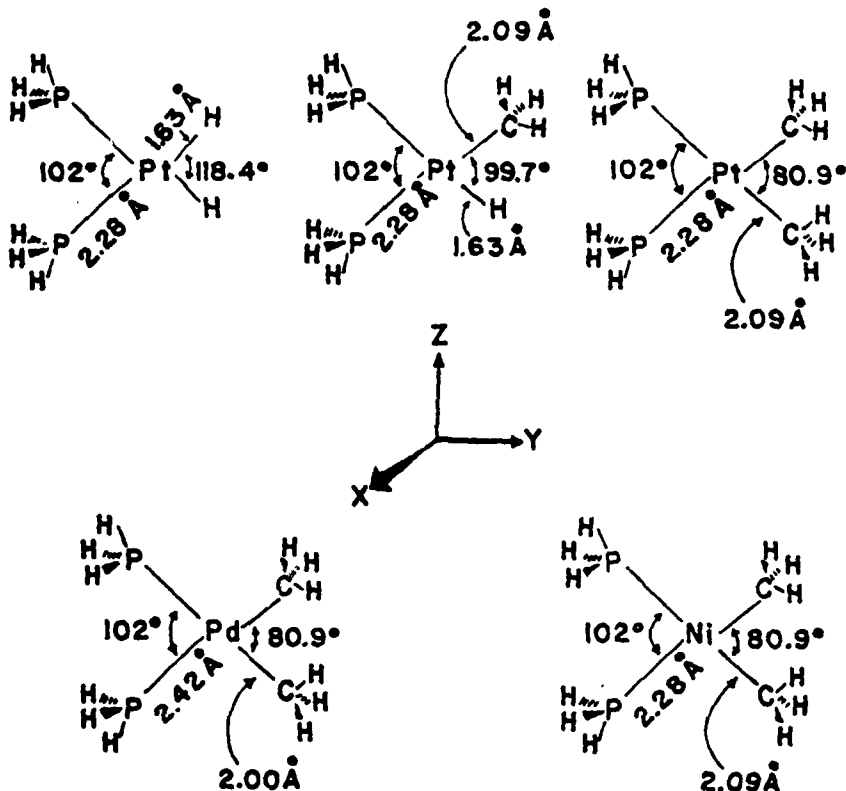
Calculations were carried out using the SCF-X $\alpha$ -SW method described elsewhere<sup>13</sup>. The general strengths and weaknesses of this method have been summarized by Salahub, et al.<sup>14</sup> Here we emphasize only points which are relevant to the particular problem being explored. The SCF-X $\alpha$ -SW method has two strengths vis à vis other theoretical methods. First, it can calculate wavefunctions and relative energies of orbitals for many-electron systems economically, and provides good wavefunctions for species characterized by pronounced ionic character in bonds. It is thus practical to use this method to examine organometallic compounds containing heavy elements such as platinum, palladium, and nickel. The ability to calculate electron distributions in orbitals is especially useful in identifying those orbitals which contribute significantly to the bonding (or anti-

bonding) of the metal to its ligands. This type of identification is not always obvious, especially when, as in the complexes examined here, bonding is distributed among several orbitals, rather than localized in one. Second, the eigenvalues generated in a calculation can be related directly to orbital electronegativity and provide a characterization of the electronic structure which is obtained with more difficulty using other methods. The relative energies of orbitals (that is, the differences in energy between them) are calculated relatively well using the SCF-X $\alpha$ -SW method, and one of the most useful applications of the method has been in the calculation of electronic absorption spectra for transition metal complexes (using the "transition state" method)<sup>13,15</sup>.

The present SCF-X $\alpha$ -SW calculations have the important weakness that they give unreliable total electronic energies of molecules. They are thus unsuitable for the calculation of potential surfaces, and for problems which require energy minimization. The type of calculation employed in this paper is not, for example, capable of estimating ground-state geometries<sup>16</sup>, and certainly cannot be used to estimate structures or energies of transition states. It cannot, therefore, calculate the quantity of most direct interest in any study of reaction rates -- that is, the difference in energy between ground and transition states (the activation energy). Efforts to use the SCF-X $\alpha$ -SW method at this level to examine problems in kinetics must thus rely on inferences based on the (known or estimated) ground state structures of the reactants and products, and on the energy, symmetries, and shapes of the orbitals of these materials. Orbital correlation diagrams have been employed as an aid in similar analyses employing other types of molecular orbital calculations. As we shall show, and in agreement with previous work<sup>9</sup>, they are relatively uninformative in the particular problem chosen here.

In order to use orbital correlation diagrams in any fashion, it is necessary to be able to calculate orbital energies with useful accuracy. The fact that the version of the SCF-X $\alpha$ -SW program used here can estimate individual orbital energies usefully but that it cannot estimate total electronic energies deserves some explanation. In order to facilitate rapid computation, an additional approximation is introduced in calculating the X $\alpha$  total energy that is not made in calculating individual orbital energies: the charge density generated from the one-electron wavefunctions is spherically averaged within the atomic sphere boundaries and assumed to be a constant in the region between the spheres. This procedure introduces major errors in the value of the total energy. Dramatic improvements of the total energy have been achieved when the full, unaveraged, charge density generated is used in evaluating the X $\alpha$  total energy<sup>16</sup>. These improvements suggest that the discrepancies between total energies calculated in the X $\alpha$ -SW model and experiment are caused mainly by the approximation of a spherical charge distribution and are not a reflection of intrinsic defects in the X $\alpha$  method.

The geometries chosen for the five complexes studied are these:



These distances and angles are unfortunately poorly based in detailed experimental precedent, but are sufficiently accurate to examine qualitative trends in the complexes involved<sup>17</sup>. In any event, these choices resemble closely those used by Hoffmann, *et al.*<sup>9</sup> in a useful study of reductive elimination, and facilitate comparison between the results of these studies.

#### Calculations

~~~~~

Schwarz's α_{HF} values¹⁸ were used for the atomic exchange parameters, except for hydrogen, for which 0.77725 was used¹⁹. For the extramolecular and intersphere regions, a weighted average of the atomic α 's was employed,

the weights being the number of valence electrons in neutral atoms. Overlapping sphere radii were used^{20,21}.

To provide a check on the consistency of the parameters used for carbon and hydrogen, the transition state method was used to calculate the first ionization potentials for dihydrogen, methane and ethane. These values, together with experimental values²², are (eV): H₂, 17.6, 15.4; CH₄, 12.7, 12.6; C₂H₆, 11.0, 11.5. A similar calculation for the metals gives (calc'd., obsd.): Pt, 8.77, 9.00; Pd, 8.57, 8.33; Ni, 7.89, 7.63^{22,23}. Using the same method, Parr, et al. have calculated the electron affinities for the elements up to atomic number 54 with a similar level of agreement²⁴. Comparison of these several experimental and calculated values suggest the values calculated by the SCF-Xa-SW method to be uncertain by about 1 eV. We place this level of agreement between calculated and experimental numbers in perspective by noting that it is unlikely that the total spread in values for ΔG^\ddagger for the reductive elimination of XY from the L₂ MXY complexes studied here exceeds 1 eV. Thus, the uncertainty in quantitative precision of the computational method is approximately the same as the magnitude of the phenomenon being studied; accordingly, only qualitative trends in the calculations are interpretable.

Atomic charges were calculated using a qualitative procedure, and are useful only for comparisons: the absolute values are not reliable²⁵. The intersphere and extramolecular charge was partitioned among the atomic centers in proportion to the intrasphere charges. That is, atomic charges were estimated by normalizing the total number of valence electrons within all the atomic spheres to the total number for the molecule. The sphere sizes for a particular element also vary slightly from compound to compound;

this variation also complicates quantitative interpretation of calculated charge distributions.

Results

~~~~~

$L_2PtH_2$ ,  $L_2Pt(H)CH_3$ , and  $L_2Pt(CH_3)_2$ . Figure 1 gives calculated eigenvalues. Only orbitals involved in bonds between P, Pt, and X(Y) (and nonbonding d orbitals on Pt) are shown; inner shell orbitals, and P-H and methyl C-H bonds are omitted. Figures 2 - 4 summarize the composition of important molecular orbitals ("important" is defined by the orbital correlation diagrams as orbitals involved in bonds which are made or broken during elimination of XY from  $L_2PtXY$ ; see below).

For comparison, Figure 5 gives similar information for  $L_2Pt(O)$ . Reductive elimination of XY from  $L_2PtXY$  with generation of  $L_2Pt(O)$  is certainly accompanied by a spreading of the L-Pt-L angle. We cannot estimate the value of this angle at the transition state. Figure 5 arbitrarily gives orbitals for an L-Pt-L bond angle of  $141^\circ$ ; Figure 6 indicates the change in these orbital energies with angle.

Classification of molecular orbitals for  $L_2PtXY$  as bonding, nonbonding, or antibonding by inspection of the wavefunctions was not always straightforward, for two reasons. First, certain wavefunctions contain significant contributions from platinum  $6s$  and  $6p$  atomic orbitals, and the internal nodes of these orbitals complicated their interpretation. These internal nodes are qualitatively most obvious around platinum in the  $4b_2$  orbital of  $(H_3P)_2PtH_2$  (Figure 2) and are due to the  $6p_y$  orbital. Although there are obvious nodes between Pt and both H and P in the electron density plot for this orbital, the Pt-H and Pt-P interactions are bonding. In other orbitals, it was not always possible to identify the origin of the nodes

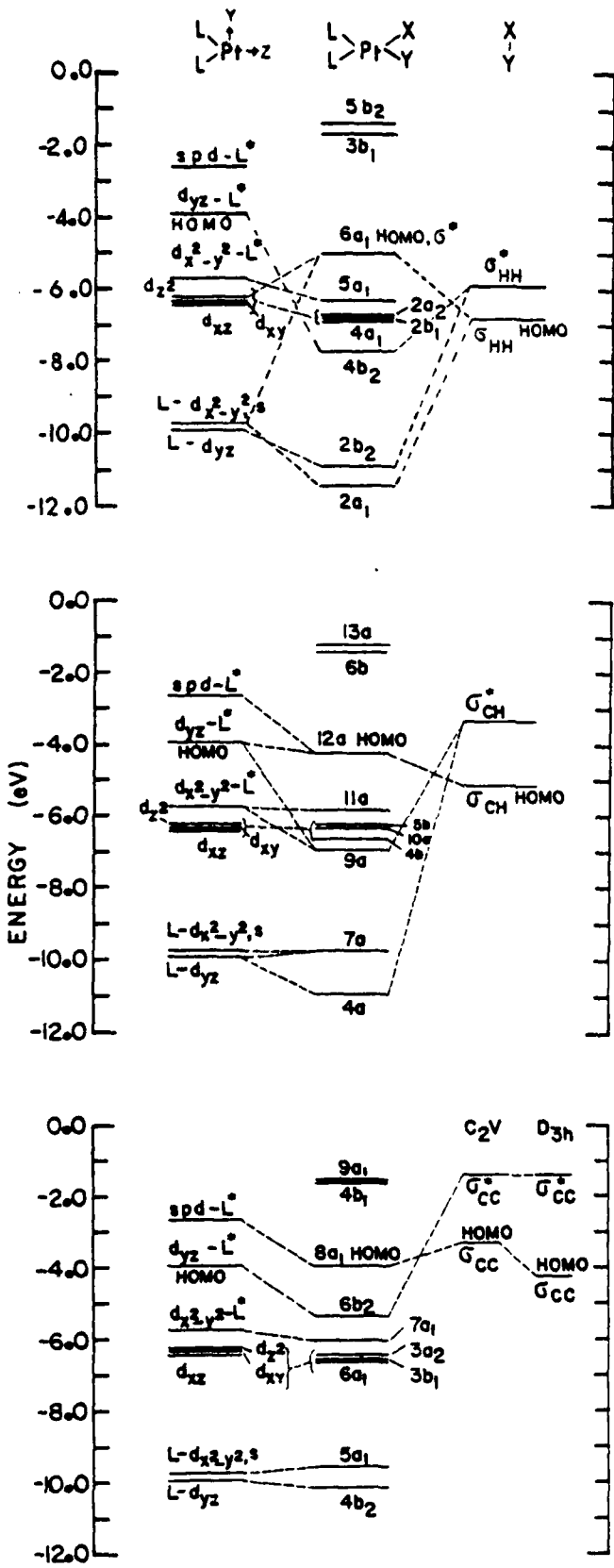


Figure 1. Eigenvalues for  $L_2PtXY$  [ $XY = HH$  (top),  $CH_3-H$  (middle),  $CH_3-CH_3$  (bottom)]. Only the orbitals of  $L_2Pt$  and  $XY$  making major contributions to the molecular orbitals of  $L_2PtXY$  are indicated. The eigenvalues for  $XY$  are those calculated at the distances assumed in the complex ( $r_{HH} = 2.80 \text{ \AA}$ ,

$r_{CH_3-CH_3} = 2.73 \text{ \AA}$ ,  $r_{CH_3-CH_3} = 2.72 \text{ \AA}$ ). In addition, the eigenvalues for  $CH_3-CH_3$  are also calculated using the bent geometry ( $C_{2v}$  symmetry) this moiety displays in the  $L_2Pt(CH_3)_2$  complex. Calculations of the distorted  $CH_3-H$  molecule displaying both  $C_{3v}$  and  $C_s$  symmetries revealed insignificant differences. The figure

displays the eigenvalues obtained from the  $CH_3-H$  fragment having  $C_{3v}$  symmetry.)  $L = PH_3$  in each case.

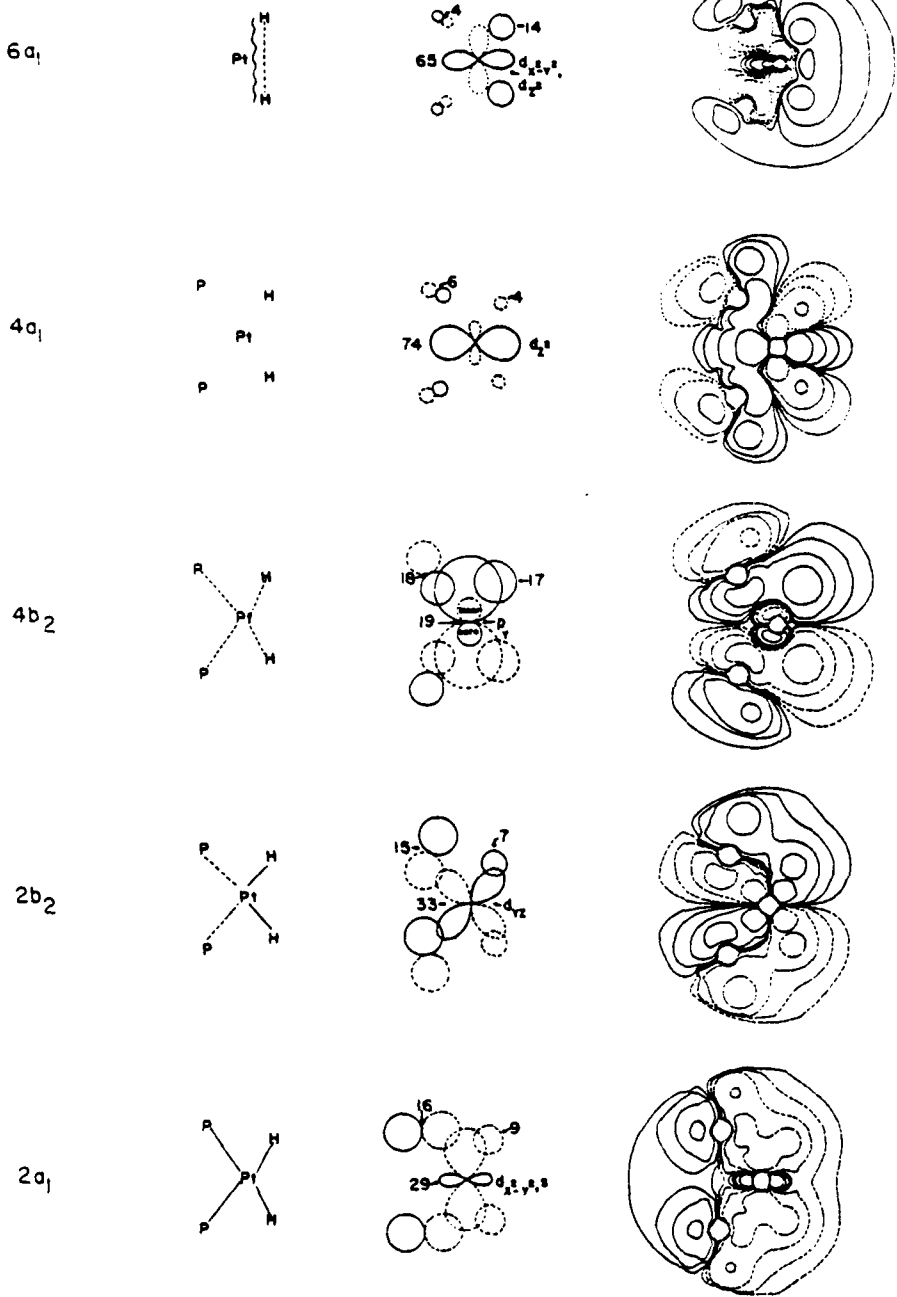


Figure 2. Orbitals important to bonding in  $L_2PtH_2$ . The first column represents the simplified interpretation of the bonding in the orbital. The representation is: — strongly bonding;  $\sim$  weakly bonding;  $\sim$  strongly antibonding. Thus, for example, the  $2b_2$  orbital has strong Pt-H bonding character and weak Pt-P bonding. The two hydrogens (and the two phosphorus atoms) are weakly antibonding with respect to one another. No line between nearest neighbor atoms (as between Pt and P in the  $4a_1$  orbital) indicates a w-t or non-bonding interaction. If a center is omitted from the diagram, the charge assigned to it is considered sufficiently small, that it effectively does not participate in the orbital. The second column sketches the orbital makeup in terms of atomic orbitals. The numbers represent the fractional charge (expressed as a percentage of two electrons) centered on each center. These charges do not add to 100 because the charge on the hydrogens in  $PH_3$  and  $CH_3$  have been omitted from the diagram. The major contributions of the orbitals on platinum are indicated on the diagram. For example, the  $2a_1$  orbital contains important contributions from  $d_{x^2-y^2}$  and  $s$  orbitals centered on platinum. The last column contains a section through the wave function. The contours are plotted at values of 0.005,  $\pm 0.009$ ,  $\pm 0.027$  and  $\pm 0.081$ , starting from the outermost.

not participate in the orbital. The second column sketches the orbital makeup in terms of atomic orbitals. The numbers represent the fractional charge (expressed as a percentage of two electrons) centered on each center. These charges do not add to 100 because the charge on the hydrogens in  $PH_3$  and  $CH_3$  have been omitted from the diagram. The major contributions of the orbitals on platinum are indicated on the diagram. For example, the  $2a_1$  orbital contains important contributions from  $d_{x^2-y^2}$  and  $s$  orbitals centered on platinum. The last column contains a section through the wave function. The contours are plotted at values of 0.005,  $\pm 0.009$ ,  $\pm 0.027$  and  $\pm 0.081$ , starting from the outermost.

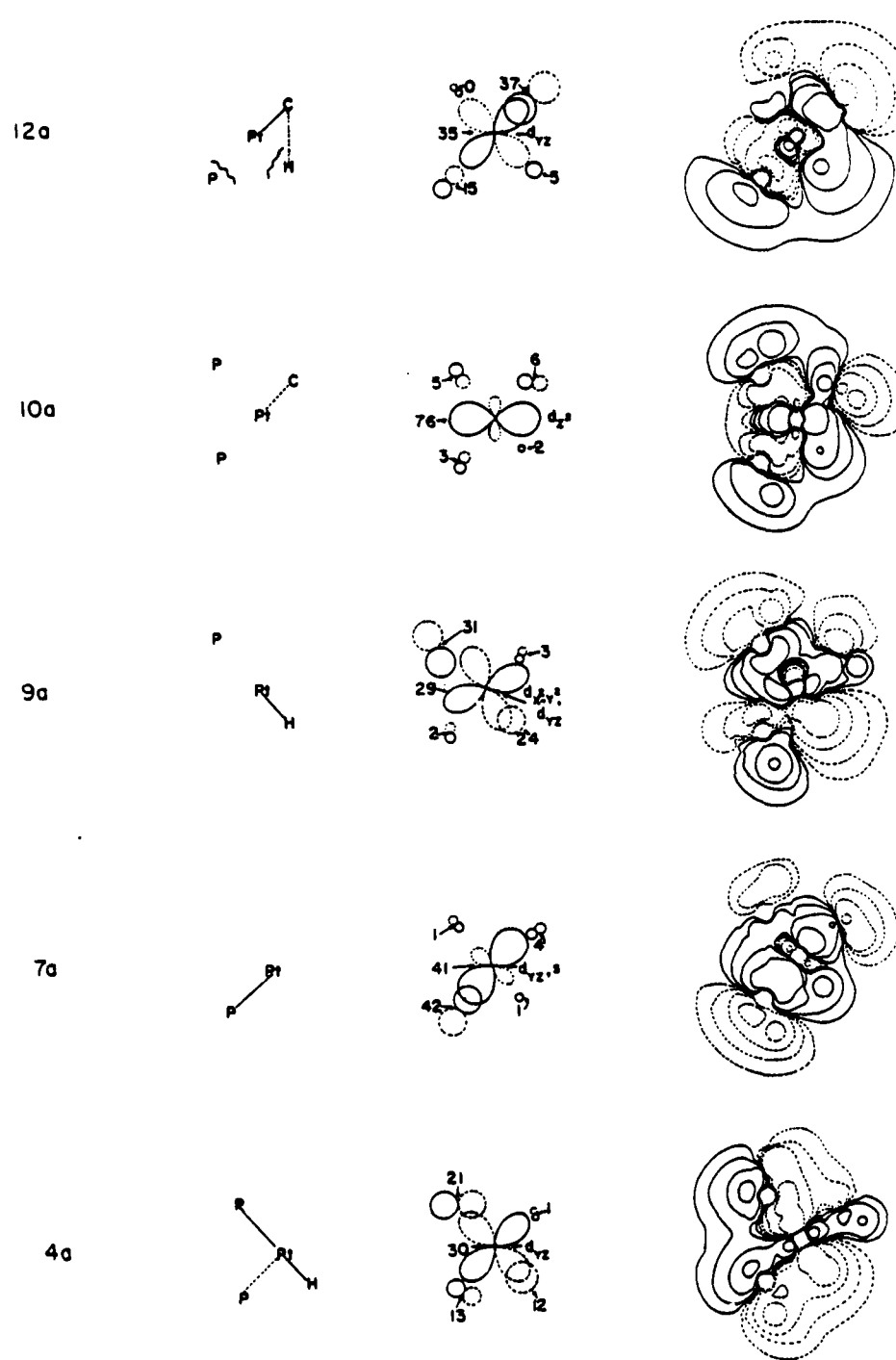


Figure 3. Orbitals important to bonding in  $L_2Pt(H)CH_3$ . The caption for Figure 2 contains nomenclature.

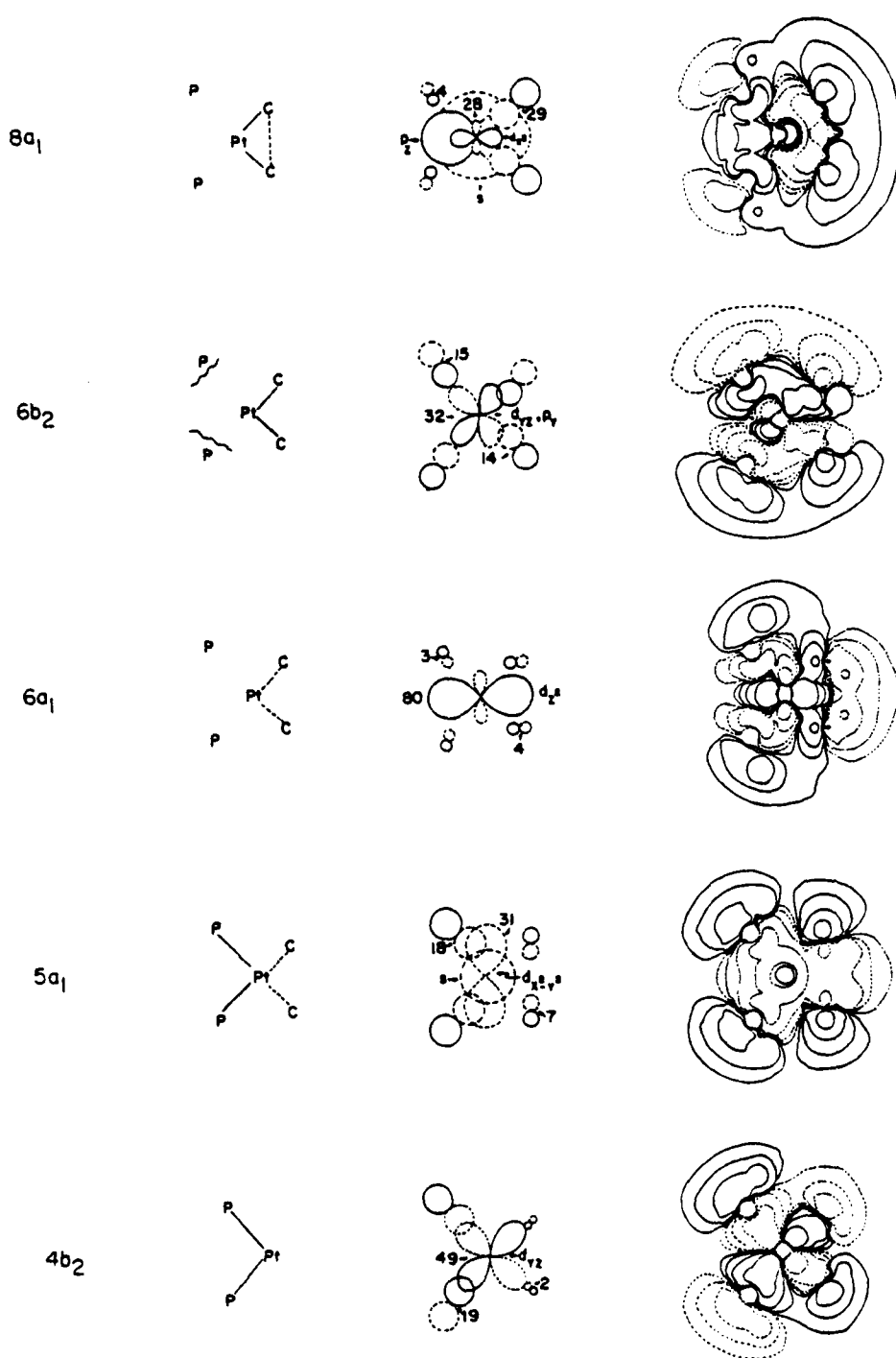


Figure 4. Orbitals important to bonding in  $L_2\text{Pt}(\text{CH}_3)_2$ . The caption for Figure 2 contains nomenclature.

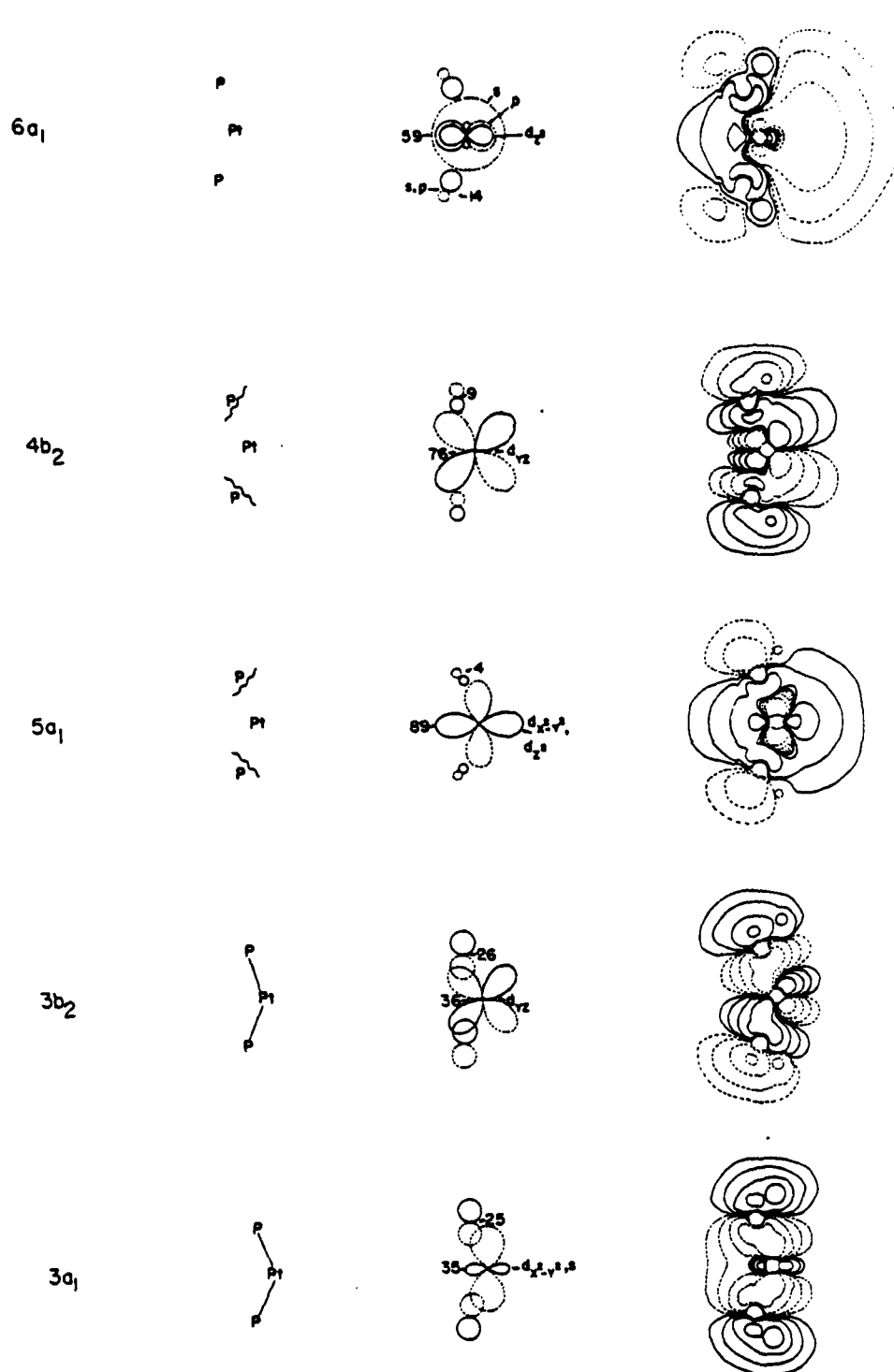


Figure 5. Orbitals for  $L_2Pt(0)$  for angle  $LPtL = 141^\circ$ . The caption for

Figure 2 contains nomenclature.

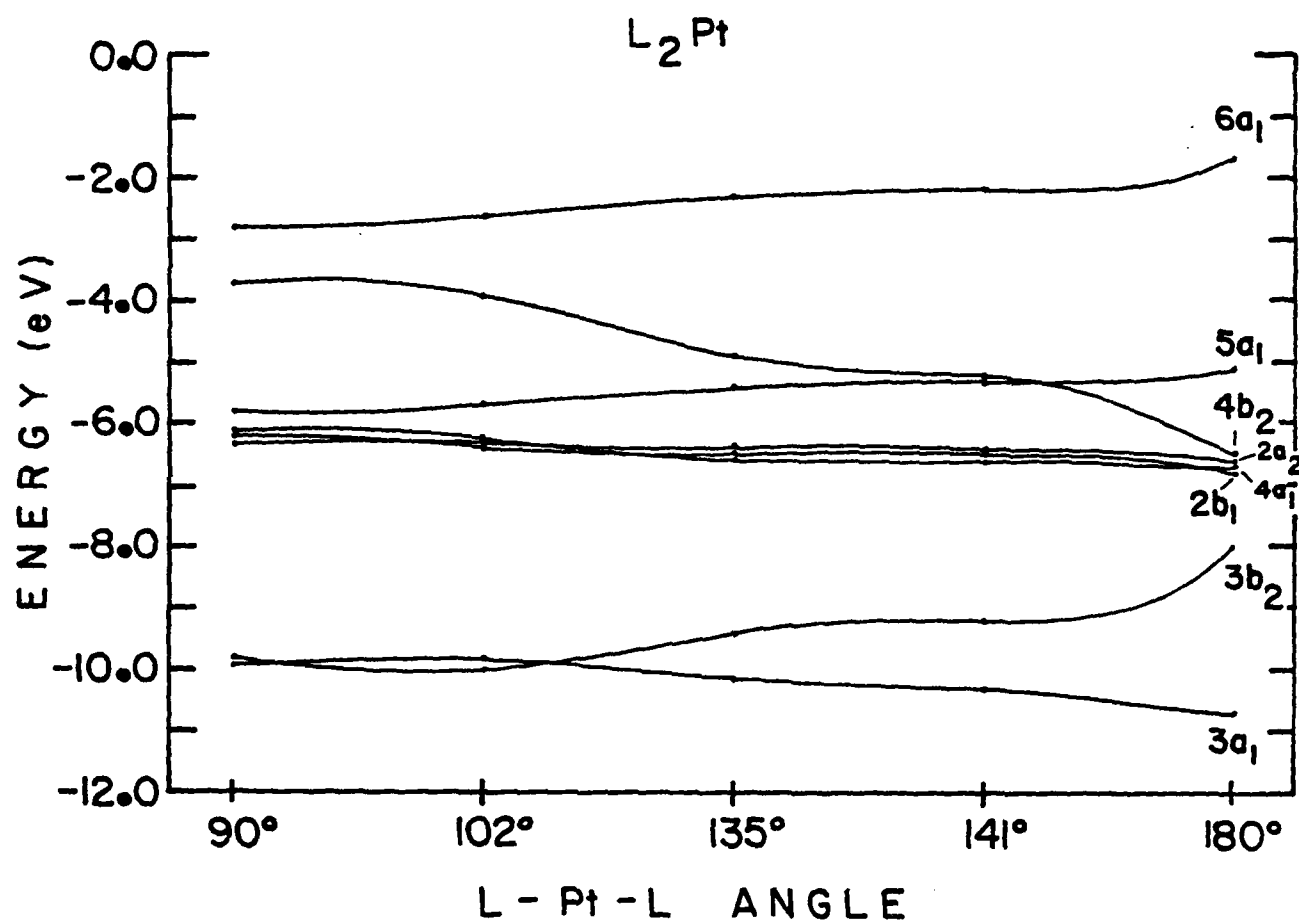


Figure 6. Eigenvalues for  $L_2 Pt(0)$  as a function of angle L Pt L.

by inspection. Second, for orbitals containing a significant contribution from the platinum  $5d_z^2$  atomic orbital, it is possible to have coexisting bonding and antibonding contributions reflecting overlap of the ligand orbital with the torus or the central lobe of the platinum-centered  $d$  orbital.

The origin and character of the nodes in these orbitals was clarified by a procedure which is illustrated in Figure 7 for  $(H_3P)_2PtH_2$ . The eigenvalues were recalculated for new geometries in which bonds of interest were selectively stretched. For example, increasing the Pt-H distance of  $L_2PtH_2$  lowers the energy of the  $6a_1$  orbital. We conclude, then, that this orbital is antibonding with respect to the platinum-hydrogen interaction. To estimate the strength of the bonding (antibonding) interaction between two nuclei, we relied on two criteria. One was the magnitude of the change in energy which accompanied a small change in bond length (Figure 7): orbitals whose energies were sensitive to these changes were considered relatively (anti)bonding. The second was the amount of charge indicated to lie between the nuclei in the contour diagrams (Figures 2-4): if these diagrams showed a significant area (volume) at the highest contour level (for example, between platinum and hydrogen in the  $2b_2$  orbital of  $L_2PtH_2$ ) the orbital was considered bonding.

Having identified the molecular orbitals responsible for bonding platinum to hydrogen and carbon in these complexes, it is possible to interpret orbital correlation diagrams describing the conversions  $L_2PtXY \rightarrow L_2Pt + XY$  (Figure 8). These calculations contain an arbitrary element: as indicated earlier, we do not know the LPtL bond angle of the  $L_2Pt$  fragment produced as a product. Orbital correlations are given for two extremes:

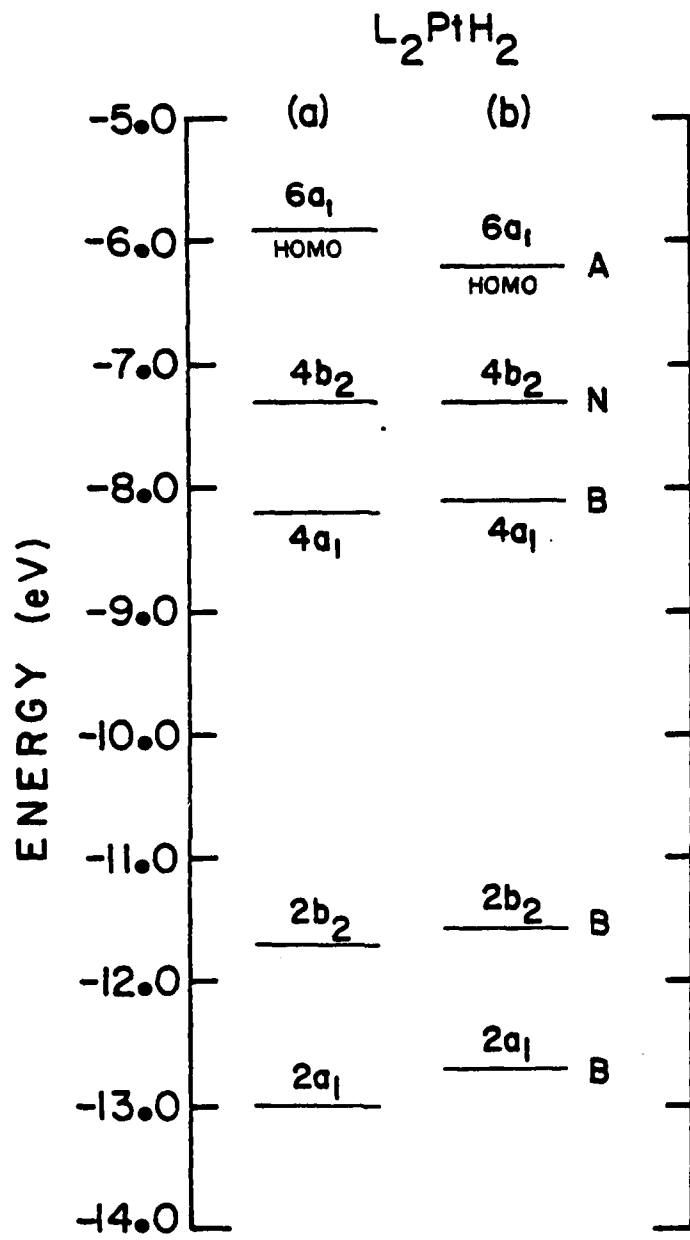


Figure 7. The response of the eigenvalues of  $L_2PtH_2$  (a) to a 10% increase in the Z-coordinate of the hydrogen atom (b). These shifts in energies were used to classify the energies as bonding (B), non-bonding (N) or antibonding (A) with respect to the Pt-H interactions.

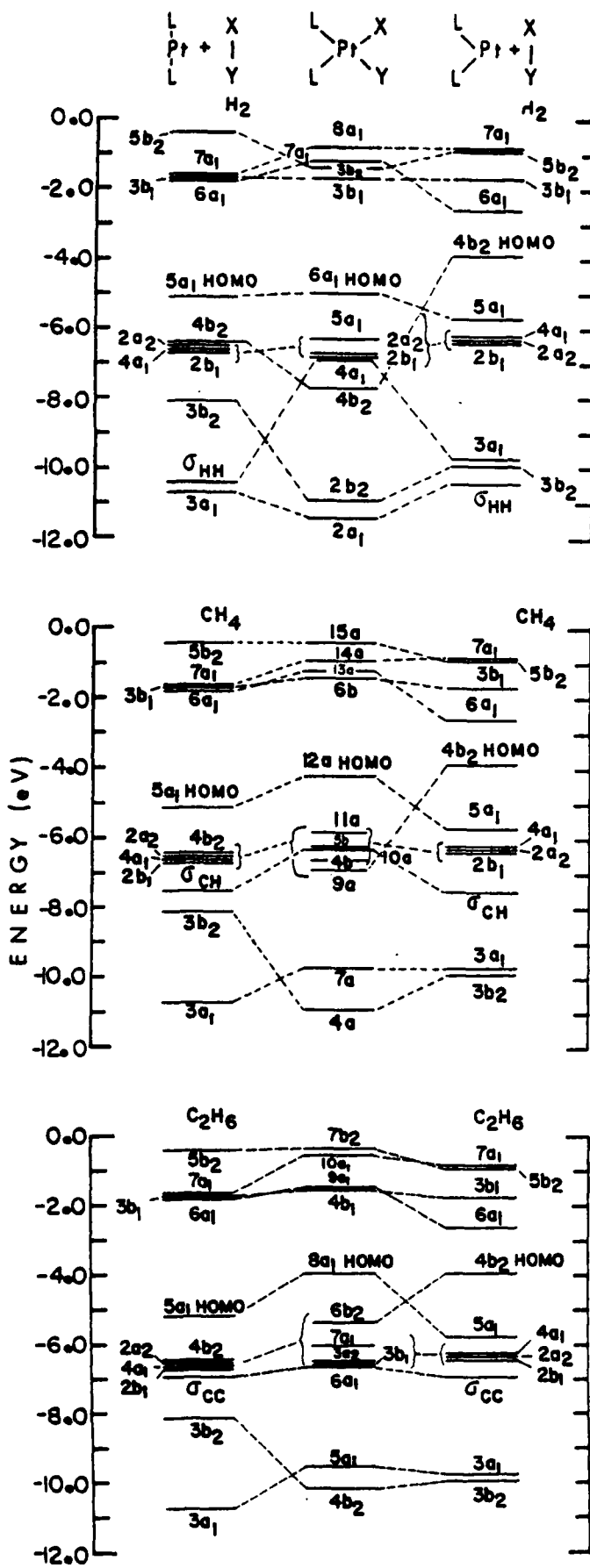


Figure 8. Orbital correlations diagrams for decompositions of  $L_2PtXY$  to  $XY$  and  $L_2Pt$  (angle = 102° and 180°).  $XY$  is in its ground-state geometry.

one having the L-Pt-L angle corresponding to the starting material ( $LLPtL \approx 90^\circ$ ) and the second to that of the final, relaxed, product ( $LLPtL \approx 180^\circ$ ). The information summarized in Figure 6 indicates that choosing another bond angle will not significantly influence the conclusions, particularly insofar as only the relative rates of decomposition of the three platinum complexes are of interest.

Figures 2-4 and the orbital correlation diagrams of Figure 8 contain several items of information relevant to the elimination of X-Y from  $L_2PtXY$ . First, the orbital correlation diagrams indicate that all three eliminations considered are allowed by orbital symmetry. Second, Figures 2-4 imply that the strength of the bonding between Pt and X(Y) is not due to a single orbital, but represents the sum of interactions in several orbitals. Third, these figures suggest a definite difference in the distribution of Pt-X(Y) bonding, nonbonding, and antibonding contributions among these orbitals. For  $L_2Pt(CH_3)_2$ , the upper orbitals have Pt-CH<sub>3</sub> bonding character and there are no occupied Pt-CH<sub>3</sub> antibonding orbitals. For  $L_2PtH_2$ , the highest occupied orbital is Pt-H antibonding, and the lower ones are Pt-H bonding. For  $L_2Pt(H)CH_3$ , an intermediate situation is observed. Thus, these Figures contain the suggestion that the relative rates of reductive elimination (that is, essentially, the relative thermal instabilities) from these complexes correlate with the occupancy of Pt-X(Y) antibonding orbitals.

$L_2Pd(CH_3)_2$  and  $L_2Ni(CH_3)_2$ . Figure 9 gives eigenvalues; Figures 10 and 11 summarize information concerning wavefunctions; Figure 12 gives orbital correlation diagrams for reductive elimination. All are given in forms analogous to those used with  $L_2Pt(CH_3)_2$ , to facilitate comparison

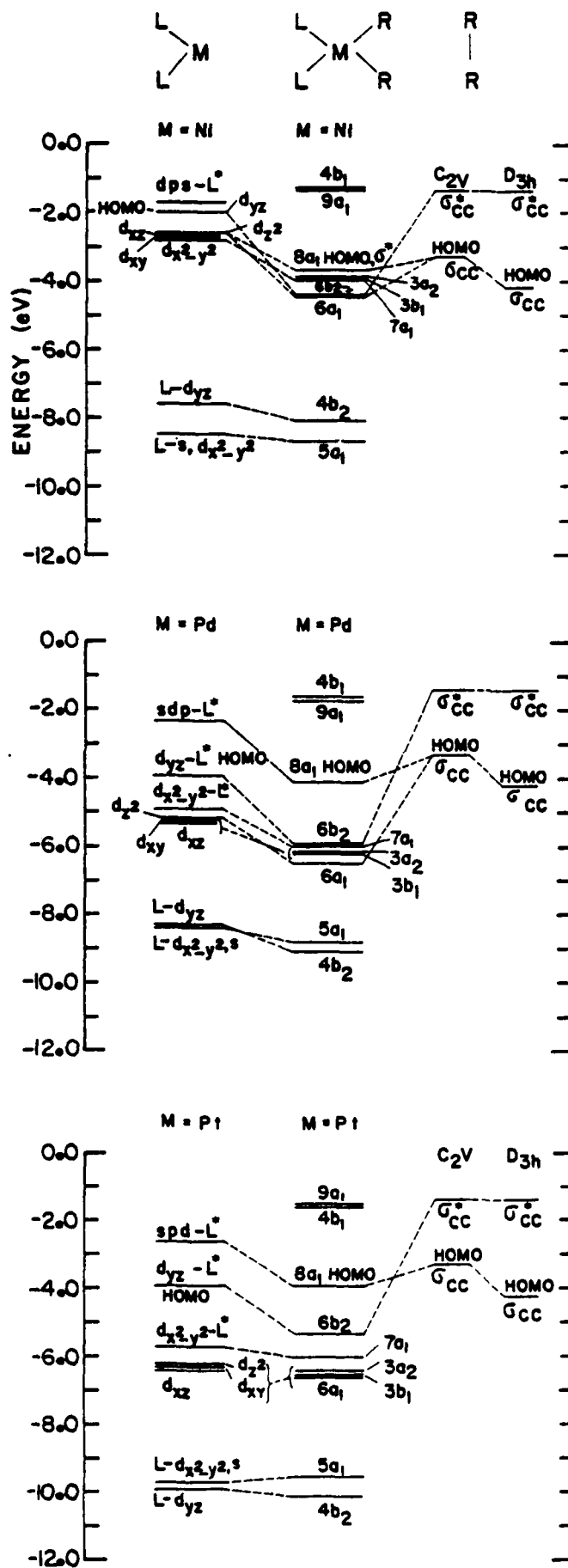


Figure 9. Eigenvalues for  $L_2M(CH_3)_2$  [ $M = Pt, Pd, Ni$ ]. Only the orbitals of  $L_2M$  making major contributions to the molecular orbitals of  $L_2M(CH_3)_2$  are indicated.  $L = PH_3$  in each instance.

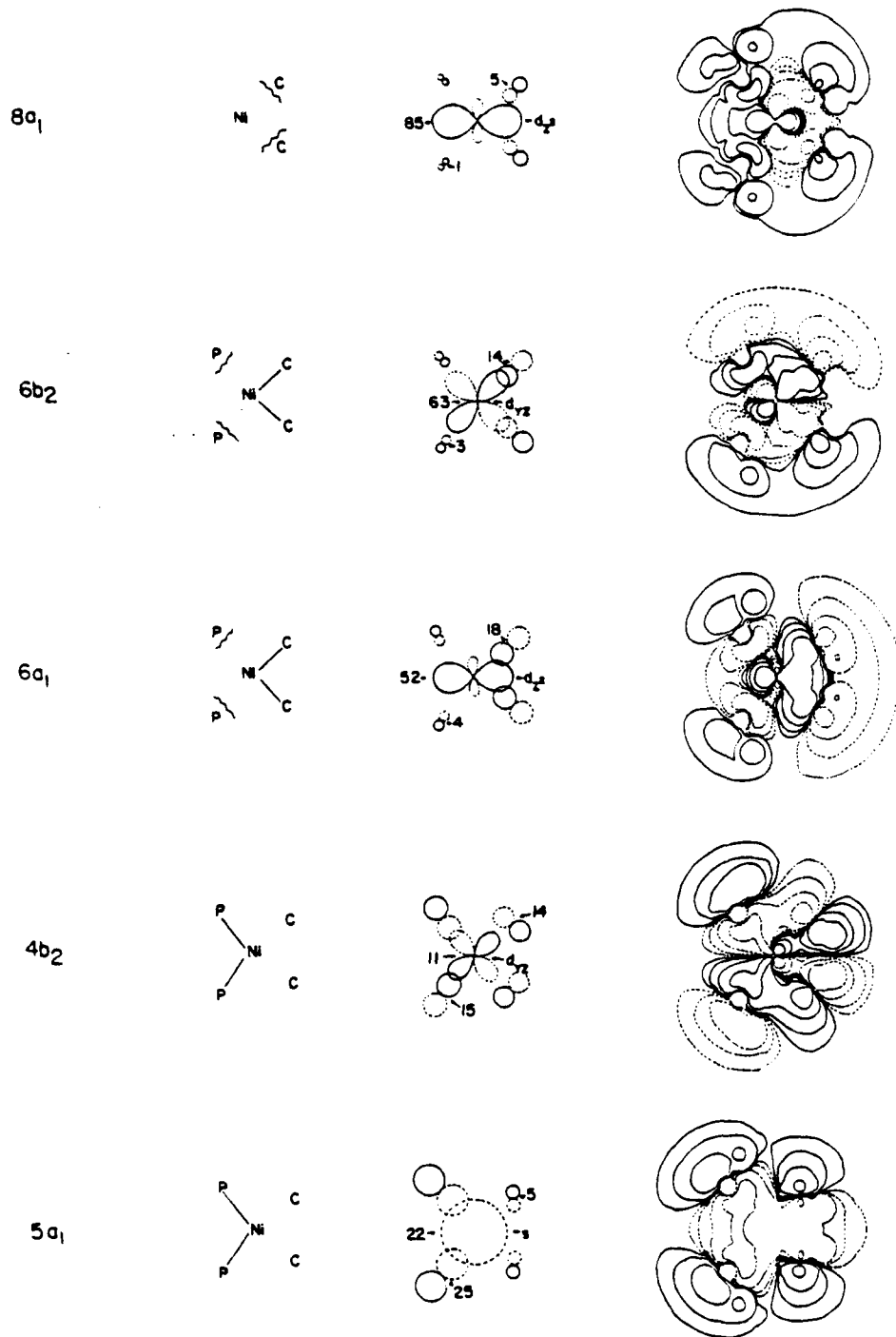


Figure 10. Orbitals important to bonding in  $L_2Ni(CH_3)_2$ . The caption for Figure 2 contains nomenclature.

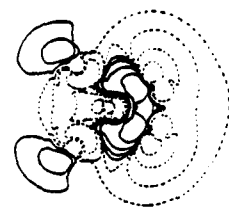
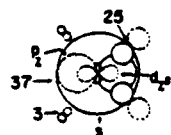
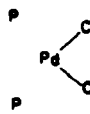
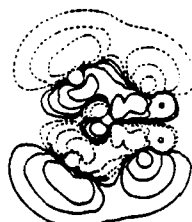
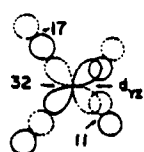
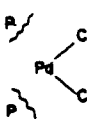
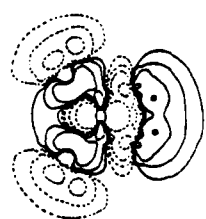
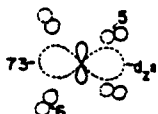
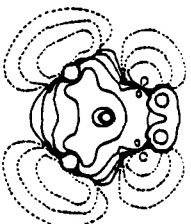
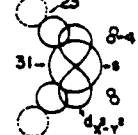
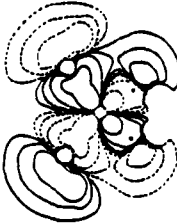
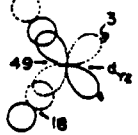
8a<sub>1</sub>6b<sub>2</sub>6a<sub>1</sub>5a<sub>1</sub>4b<sub>2</sub>

Figure 11. Orbitals important to bonding in  $L_2Pd(CH_3)_2$ . The caption for Figure 2 contains nomenclature.

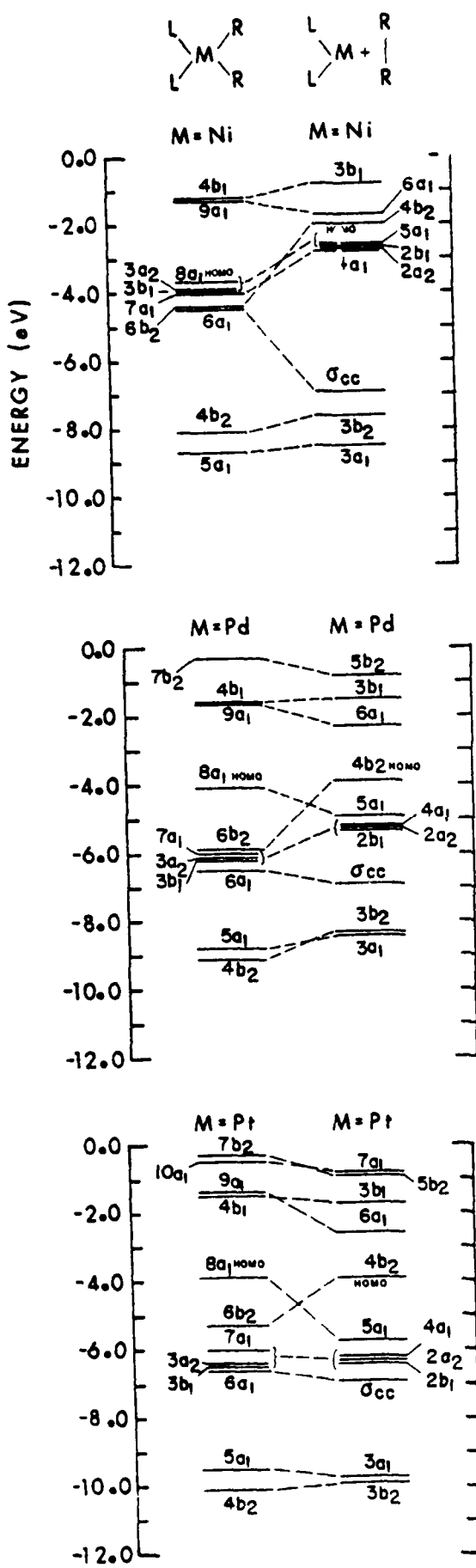
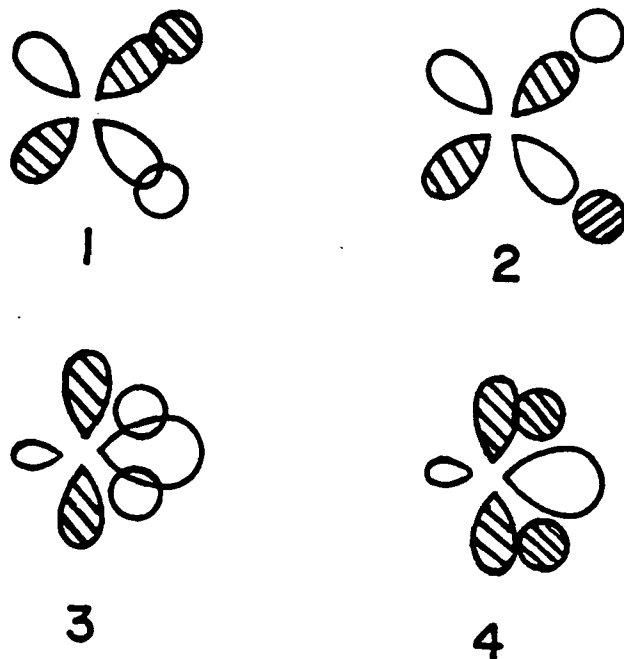


Figure 12. Orbital correlation diagrams for decomposition of  $L_2M(CH_3)_2$  to  $C_2H_6$  and  $L_2M$  (angle =  $102^\circ$ ).  $C_2H_6$  is in its ground-state geometry.

The inferences from the calculations for  $L_2Pd(CH_3)_2$  and  $L_2Ni(CH_3)_2$  are similar to those for the platinum complexes. The orbital correlation diagrams indicate that all of the reactions are allowed by orbital symmetry. Examination of the occupied orbitals indicates that the HOMO of  $L_2Ni(CH_3)_2$  (the  $8a_1$  orbital) is weakly antibonding with respect to the C-Ni bond (the orbital is predominantly a nickel  $d_z^2$  orbital, with relatively little electron density on carbon). The orbitals of  $L_2Pd(CH_3)_2$  and  $L_2Pt(CH_3)_2$  are qualitatively indistinguishable: neither has identifiable occupied M-C antibonding orbitals.

Discussion

The bonding between M and X(Y) in  $L_2MXY$  seems to be distributed among a number of orbitals of similar energies. To the extent that the rates of reductive elimination from these complexes are determined by their electronic structure, these rates are not expected to be entirely controlled by the properties of the HOMO, or by orbital symmetry considerations, but rather by the collective action of several valence orbitals. Nonetheless, a limited number of these orbitals undoubtedly are particularly important. Orbitals with the character of  $1$  or  $2$  are clearly important bonding and antibonding orbitals; molecular orbitals formed from combinations of  $d_z^2$ ,  $d_{x^2-y^2}$ ,  $s$ , and  $p$  atomic orbitals on the metal ( $3,4$ ) also appear from the orbital contour diagrams to be able to contribute significantly to bonding or antibonding.



One clear correlation emerges from this work relating molecular orbital structure to rates of reductive elimination. Compounds which decompose rapidly ( $L_2PtH_2$ ,  $L_2Ni(CH_3)_2$ ) have occupied orbitals with antibonding M-X character; compounds which decompose slowly ( $L_2Pt(CH_3)_2$ ) have occupied M-X bonding orbitals and vacant M-X antibonding orbitals. In the simplest terms, this correlation is almost trivial: it implies that compounds in which the M-X(Y) bonds are weak, decompose more rapidly than those in which these bonds are strong<sup>22</sup>. The interesting question then becomes: what is the basis in atomic or molecular structure for the changes in molecular electronic structure which are reflected in the occupancy of antibonding orbitals?

We hypothesize that the difference between the energies of the interacting orbitals of M and X(Y) is one determinant. Figure 13 summarizes the argument which forms the basis for this hypothesis in a highly simplified and schematic way. Consider a group of orbitals for the  $L_2Pt$  moiety ( $L \approx 90^\circ$ ) of  $L_2PtX_2$ , and the  $\sigma_g$  HOMO (a symmetry) for the  $X_2$  moiety. Assume, for simplicity, that the  $\sigma_g$  orbital interacts only with the  $L_2Pt$  of the correct symmetry closest to it in energy. (Strong interaction between orbitals of similar energies is usually rationalized on the basis of orbital size and overlap<sup>26</sup>. In this instance, since Pt and H or  $CH_3$  have somewhat different orbital sizes, this assumption is not strictly justifiable. Nonetheless, the qualitative argument remains.) If it is an occupied orbital (of the correct symmetry for overlap) of the  $L_2M$  complex which matches the  $\sigma_{X_2}$  orbital most closely in energy, the resulting M-X bonding and antibonding orbitals may both be occupied (Figure 13A, exemplified by  $L_2PtH_2$  and  $L_2Ni(CH_3)_2$ ). If it is an unoccupied  $L_2M$  orbital which lies closest in energy to  $\sigma_{X_2}$  (Figure 13B,  $L_2Pt(CH_3)_2$ ,  $L_2Pd(CH_3)_2$  or if the HOMO of  $L_2M$  interacts strongly with  $\sigma_{X_2}^*$  (Figure 13C; note the  $6b_2$  level in  $L_2Pt(CH_3)_2$ ) the  $\sigma_{MX_2}^*$  orbitals resulting from these interactions should be vacant. Thus, in brief, if the orbital electronegativities are similar for  $\sigma_{X_2}$  and the highest-lying  $L_2M$  orbital of the same symmetry, the  $MX_2$  fragment can be expected to have an occupied antibonding orbital and to be unstable with respect to reductive elimination; if these orbital electronegativities are enough different that one of the strongly-interacting pair of high-lying orbitals is vacant, the  $MX_2$  fragment should have a vacant antibonding orbital and be relatively stable to reductive elimination. In other terms, the interaction suggested by Figure 13A is predominantly covalent while that in

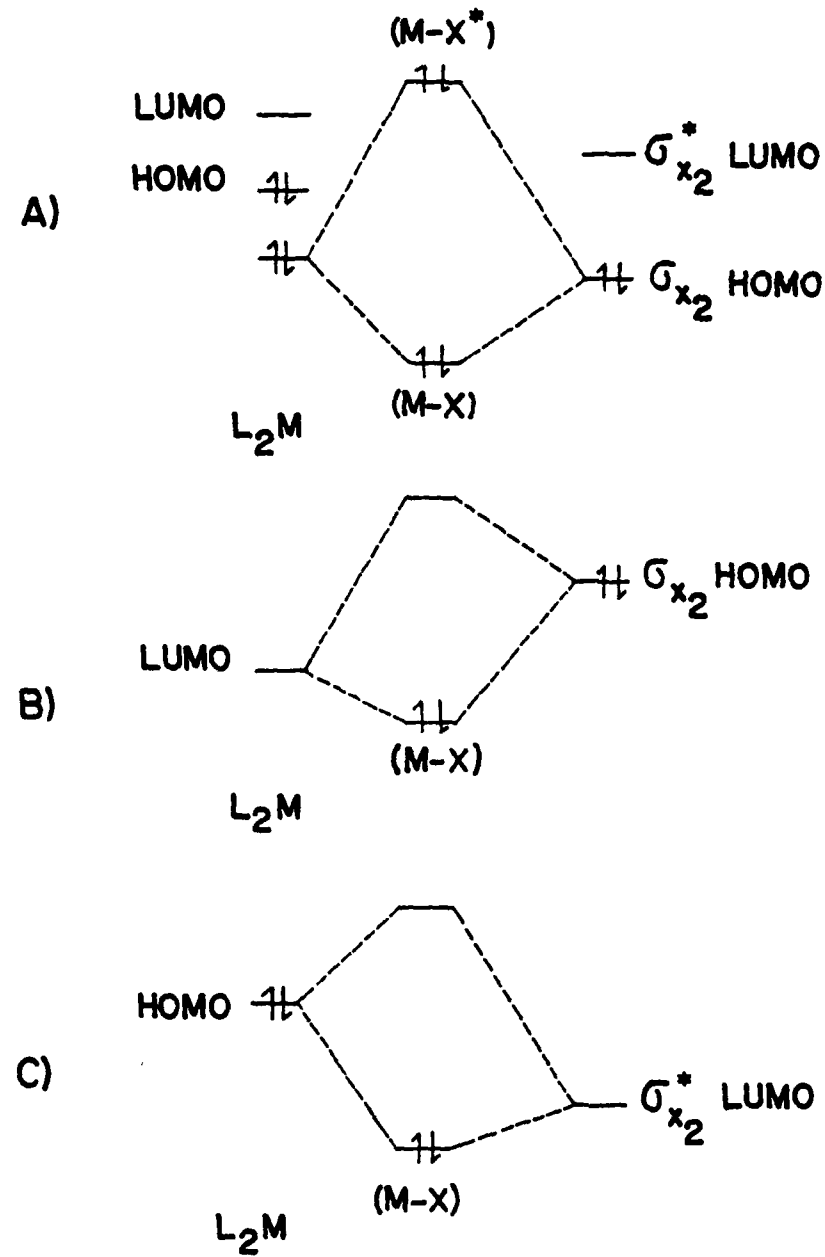


Figure 13. A schematic energy level diagram summarizing the important interactions in  $L_2MXY$ .

Figures 13B and 13C has more or less ionic character.

Reference to Figures 2, 4, 10 and 11 indicate that the important elements in these orbital correlation diagrams are approximated by the interactions outlined in Figure 13, although they are obviously more complicated, since several  $L_2M$  orbitals have the correct symmetry to interact with  $\sigma_{X_2}$  and  $\sigma_{X_2}^*$ .

Inspection of calculated charges in the several complexes examined here supports these hypotheses concerning the importance of electronegativities (Table 1). For the series  $L_2M(CH_3)_2$ , the complex in which the least charge transfer from carbon to metal would take place during reductive elimination is  $L_2Ni(CH_3)_2$ ; this complex is also the one for which reductive elimination is most rapid. For the series  $L_2PtXY$ , the complex for which the least charge is transferred to the metal during reductive elimination is  $L_2PtH_2$ . This complex is also the one which reductively eliminates most rapidly of the series containing platinum.

This model correlates the rates of reductive elimination with the presence of occupied  $M-X(Y)$  antibonding orbitals, and by inference with the relative orbital electronegativities of the  $L_2M$  orbitals and the "stretched"  $\sigma_{XY}$  orbital. It hypothesizes that the relative electronic energies of the starting materials determine the rates of these reductive elimination reactions. A number of other possible models for these reactions might, of course, also be considered. Several of these follow. We note that each of the factors emphasized in these models undoubtedly contributes to some extent to the rates of these reactions and that they are not necessarily orthogonal.

Table I Calculated Atomic Charges in Complexes of the Structure  $L_2PtXY$

( $L = PH_3$ ,  $X, Y = H, CH_3$ )

| Complex               | P      | M      | C      | H                   |
|-----------------------|--------|--------|--------|---------------------|
| $L_2PtH_2$            | +0.28  | -0.20  |        | -0.04               |
| $L_2PtHCH_3$          | +0.298 | -0.160 | -0.107 | -0.024              |
| $L_2Pt(CH_3)_2$       | +0.28  | -0.001 | -0.176 |                     |
| $L_2Pd(CH_3)_2$       | +0.27  | -0.061 | -0.140 |                     |
| $L_2Ni(CH_3)_2$       | +0.44  | -0.59  | -0.013 |                     |
| $H_2$                 |        |        |        | 0.0                 |
| $(H_c)_3C-H$          |        |        | +0.174 | -0.129 <sup>a</sup> |
| $C_2H_6$ <sup>b</sup> |        |        | +0.177 | -0.067              |
| $L_2Pt(90^\circ)$     | +0.393 | -0.439 |        |                     |
| $L_2Pt(102^\circ)$    | +0.403 | -0.460 |        |                     |
| $L_2Pt(180^\circ)$    | +0.422 | -0.521 |        |                     |
| $L_2Pd(102^\circ)$    | +0.525 | -0.559 |        |                     |
| $L_2Ni(102^\circ)$    | +0.372 | -0.601 |        |                     |

<sup>a</sup>The value for  $H_c$  is +0.013. The C-H distance assumed is 2.73  $\text{\AA}$ , and corresponds to the stretched value in  $L_2Pt(H)CH_3$ . <sup>b</sup>The assumed C-C distance is 2.72  $\text{\AA}$ , and corresponds to the value in  $L_2Pt(CH_3)_2$ .

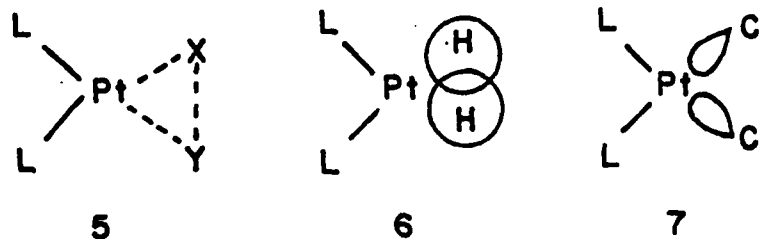
1) Exothermicity. The reaction rate for the decomposition of  $L_2MXY$  might correlate with the free energies of these reactions: such correlations are numerous in kinetics, although they usually apply only to a restricted range of variations in the reactant<sup>27</sup>. The arguments presented in this paper deal with only one contribution to this free energy: viz, the enthalpy of the reactants. The enthalpies of the products are the second contributor, and we observe that the bond energies of the products (kcal mol<sup>-1</sup>):  $D_{H-H} = 111 > D_{C-H} = 99 > D_{C-C} = 83$ ) also correlate with the rates of decomposition of  $L_2PtXY$ . The relative rates of decomposition might, in principle, be dominated by the relative energies of either the starting materials or the products. The data needed to identify the more important contributor are not available in the series examined here. Nonetheless, comparison of our results with those obtained by Hoffmann et al.<sup>9</sup> using extended Hückle methods suggests that in at least some areas the response of the transition state to changes in structure may be more like that of products than reactants (see below).

2) Relief of Steric Strain. Changes in nonbonded interactions within crowded transition metal complexes are known to be of major importance in determining the rate of many organometallic reactions, including reductive eliminations and oxidative additions<sup>2,8</sup>. The differences in size of H and  $CH_3$ , and of Pt(II), Pd(II), and Ni(II), could in principle result in contributions to rates from nonbonded interactions between X(Y) and L larger than those due to differences in bond energies.

3) Electronic Effects of Particular Importance in the Transition State. Of the many such effects which could be imagined a priori, one in particular is suggested by the contour diagrams of Figures 2 - 4. During reductive elimination, the X-Y group forms a bond. The 1s orbital on hydrogen is spherically symmetrical; the p (or  $sp^3$ ) orbitals on carbon are not. Thus, three-center

bonding of the type 5 might be more important for hydrogen (6) than methyl (7).

The  $6a_1$  of  $L_2PtH_2$  shows some evidence of H-H bonding



in the ground state; a corresponding concentration of charge between the carbon atoms of  $L_2Pt(CH_3)_2$ , or between the carbon and hydrogen of  $L_2Pt(H)CH_3$ , is not evident.

Brief comparison of our results with those of Hoffmann, et al.<sup>9</sup> is useful. Hoffmann reached three major conclusions: (1) The more strongly electron donating is X (and Y), the more rapid is reductive elimination; (2) The more strongly electron donating is L, the slower is reductive elimination; (3) The barrier to reductive elimination is determined in major part by  $b_2$  orbitals of type 1. The first two of these conclusions have some experimental support. In general, the complexes  $L_2MX_2$  are more stable for  $X = CF_3^{28}$ , Cl, Ph than for  $X = CH_3$ ; Halpern, et al. have reported that the rate of loss of methane from  $(X-Ph_3P)_2Pt(CH_3)H$  is more rapid when X is electron-withdrawing. Our calculations apply only to the electronic structures of the reactants.

A large (several eV) lowering in the energy of the X(Y) orbitals, or a large increase in the energy of the  $L_2M$  orbitals should increase the probability that  $PtXY$  antibonding orbitals are occupied, and predict a destabilization of the complexes. The influence of small changes of the type encountered in substituents is not obvious. Qualitatively, since charge density on the metal center of  $L_2M$  is larger than that in  $L_2MXY$ , electron donating L should destabilize the product more than the reactant. Similarly, since reductive elimination involves charge transfer from X(Y) to metal, the more electron-withdrawing X(Y), the more stable should be  $L_2MXY$ . Thus, the results of our studies provide an adequate ad hoc rationalization of observed substituent effects, and can be interpreted to be consistent with the potential surfaces calculated by Hoffmann, et al. They do not, however, lend themselves easily to predictions of rate differences resulting from small perturbations in substituent structure. The third conclusion of Hoffmann, that the energy of an orbital of type I dominates the changes in energy in going from reactant to transition state, cannot be compared with our results, since we do not calculate total energies.

Acknowledgments. This work was supported by NSF (DMR-78-24185) and the Office of Naval Research.

Notes and References

1. Gates, B. C.; Katzer, J. R.; Schmit, G. C. A., Chemistry of Catalytic Processes, McGraw-Hill, New York, 1979. Webster, D. E., Advan. Organometal. Chem., 1977, 15, 147-188. Sinfelt, J. H., Science, 1977, 195, 641-646. Clarke, J. K. A.; Rooney, J. J., Advan. Catal., 1976, 25, 125-183. Parshall, G. W. Homogeneous Catalysis, Wiley-Interscience, New York, 1980.
2. Pt: McCartney, T. J.; Nuzzo, R. G.; Whitesides, G. M., J. Am. Chem. Soc. 1981, 103, 0000. Young, G. B.; Whitesides, G. M., ibid. 1978, 100, 5808-5815. Foley, P.; DiCosimo, R.; Whitesides, G. M., ibid., 1980, 102, 6713-6725. Abis, L.; Sen, A.; Halpern, J., ibid., 1978, 100, 2915-2916. Braterman, P. S.; Cross, R. J.; Young, G. B., J. Chem. Soc. Dalton, 1976, 1306-1310, 1310-1314.
3. Pd: Ozawa, F.; Ito, T.; Yamamoto, J. Am. Chem. Soc., submitted; Milstein, D.; Stille, J. K., ibid. 1979, 101, 4981-4991; Gillie, A.; Stille, J. K., ibid., submitted.
4. Ni: Grubbs, R. H.; Miyashita, A., J. Amer. Chem. Soc., 1978, 100, 7416-7418; 7418-7420. Yamamoto, T.; Yamamoto, A., Ikeda, S. ibid 1971, 93, 3350-3359; 3360-3364.
5. Other possible processes which might result in reductive elimination include free radical pathways (Whitesides, G. M.; Bergbreiter, D.; Kendall, P. E. J. Am. Chem. Soc. 1976, 96, 2806-2813. Kochi, J. K. in Free Radicals, Vol. 1, Wiley Interscience, New York, 1973, Chapter 11), bimolecular processes or cluster processes (Norton, J. R. Accounts Chem. Res. 1979, 12, 139-145 and references cited therein); electron transfer reactions (Tsou, T. T.; Kochi, J. K. J. Am. Chem. Soc. 1978, 100, 1634-1635); paths requiring prior oxidative addition (Brown, M. P.; Puddephatt, R. J.; Upton, C. E. E. J. Chem. Soc. Dalton, 1974, 2456-2465.) and reactions involving compositions and geometries different

from the ground state (Grubbs, R. H.; Miyashita, A.; Liu, M.; Burk, P. J. Am. Chem. Soc. 1978, 100, 2418-2425. Glockling, F.; McBride, T.; Pollock, R. J. I. J. Chem. Soc. Chem. Comm. 1973, 650 and ref. 2-4).

6. Komiya, S.; Albright, T. A.; Hoffmann, R.; Kochi, J. K. J. Am. Chem. Soc. 1976, 98, 7255-7265.

7. Benson, S. W., "Thermochemical Kinetics", John Wiley and Sons, New York, 1968, Chapter 3.

8. Tolman, C. A. Chem. Rev. 1977, 77, 313-348.

9. Tatsumi, K.; Hoffmann, R.; Yamamoto, A.; Stille, J. K. Bull. Chem. Soc. Japan in press. Hoffmann, R. Science, submitted. Gillie, A., Stille, J. K. J. Am. Chem. Soc. 1980, 102, 4933-4937.

10. Braterman, P. S.; Cross, R. J. Chem. Soc. Rev. 1973, 2, 271-294.

11. Akerman, B.; Ljungquist, A. J. Organomet. Chem. 1979, 182, 59-75.  
Akerman, B.; Johansen, H.; Roos, B.; Wahlgren, U. J. Am. Chem. Soc. 1979, 101, 5876-5883.

12. Anderson, A. B. J. Am. Chem. Soc. 1978, 100, 1153-1159. Upton, T. H.; Goddard, W. I. ibid. 1978, 100, 321-323. Rapé, A. K.; Goddard, W. A. ibid. 1977, 99, 3966-3968.

13. Slater, J. C.; Johnson, K. H. Phys. Rev. 1972, 85, 844-853. Johnson, K. H. Ann. Rev. Phys. Chem. 1975, 26, 39-57. Slater, J. C., "The Self-Consistent Field for Molecules and Solids," Vol. 4 of "Quantum Theory of Molecules and Solids", McGraw-Hill, New York, 1974, p. 101 ff. Johnson, K. H., Advan. Quantum Chem. 1973, 7, 143-185.

14. Salahub, D. R.; Foti, A. E.; Smith, V. H. J. Am. Chem. Soc. 1978, 100 7847-7859.

15. Noddeman, L. J. Chem. Phys. 1976, 64, 2343-2349.

16. Danese, J. B.; Connally, J. W. D. J. Chem. Phys. 1974, 61, 3063-3070.  
Danese, J. B.; ibid., 1974, 61, 3071-3080. Cook, M., Ph.D., Harvard University, unpublished.

17. The  $r_{PtP}$  and  $PPtP$  angle used were taken from  $(Ph_3P)_2Pt(PhC\equiv CPPh)$  (Glanville, J. O.; Steward, J. M.; Grim, S. O., J. Organometal Chem., 1967, 7, P9-P10);  $r_{PH}$  and  $HPH$  angle were from  $Ph_3$  (Sirvetz, M. H.; Weston, R. E. Jr., J. Chem. Phys., 1953, 21, 898-902). These same dimensions were used in  $L_2PtH_2$ ,  $L_2Pt(CH_3)_2$ ,  $L_2Pt(H)CH_3$  and  $L_2Ni(CH_3)_2$ . The value of  $r_{PtH}$  was taken to be the sum of platinum and hydrogen covalent radii (1.35 $\text{\AA}$ , 0.28 $\text{\AA}$ ) (Frenz, B. A.; Ibers, J. A., in "Transition Metal Hydrides", Muetterties, E. L., ed., Dekker, New York, 1971. p. 33). The  $r_{HH}$  was taken as the sum of the ionic radii (1.40 $\text{\AA}$ ) (Libowitz, G. G., "The Solid-State Chemistry of Binary Metal Hydrides," Benjamin, New York, 1965, p. 7; Ladd, M. F. C., Theor. Chem. Acta, 1968, 12, 333-336). This choice yields for the  $HPtH$  angle 118.4°. The  $r_{PtC}$  was the average  $r_{PtC}$  in  $(Ph_3P)_2\overline{Pt(CH_2)_3}CH_2$  (Biefield, C. G.; Eecle, H. A.; Grubbs, R. H., Inorg. Chem. 1973, 12, 2166-2170); the  $CPtC$  angle was also taken from this complex. The bond lengths in  $L_2Ni(CH_3)_2$  were taken as the same as those of  $L_2Pt(CH_3)_2$ , in the absence of close analogy. Similar distances and angles are seen in related complexes (Jolly, P. W.; Wilke, G., "The Organic Chemistry of Nickel" Vol. 1, Academic Press, New York, 1974, p. 197; Cook, C. D.; Koo, C. H.; Nyburg, S. C.; Shiomi, M. T., J. Chem. Soc. Chem. Comm. 1967, 426-427). The  $r_{PdC}$  and  $r_{PdP}$  bond lengths were from Mathis (Mathis, P. M., "The Organic Chemistry of Palladium," Vol. 1, Academic Press, New York, 1971, p. 39). Angles in  $L_2Pd(CH_3)_2$  were the same as those in  $L_2Ni(CH_3)_2$ .

18. Schwarz, K. Phys. Rev. B. 1972, 5, 2466-2468. Schwarz, K. Theor. Chim. Acta. 1974, 34, 225-231.
19. Slater, J. C. Int. J. Quantum Chem. 1973, 7S, 533-544.
20. Norman, J. G. Jr. J. Chem. Phys. 1974, 61, 4630-4635.  
Norman, J. G. Jr. Mol. Phys. 1976, 31, 1191-1198.
21. Atomic and outer-shpere radii (Bohrs).  $\text{Pt}(\text{PH}_3)_2$ : Outer, 7.620; Pt, 2.522; P, 2.208; H, 1.440.  $(\text{PH}_3)_2\text{PtH}_2$ : Outer, 7.878; Pt, 2.522; H, 1.440; P, 2.208. Hp, 1.440.  $(\text{PH}_3)_2\text{Pt}(\text{CH}_3)\text{H}$ : Outer, 7.620; Pt, 2.530; H, 1.460; C, 1.770; H<sub>C</sub>, 1.250; P, 2.330; Hp, 1.440.  $(\text{PH}_3)_2\text{Pt}(\text{CH}_3)\text{H}$ : Outer, 7.620; Pt, 2.530; H, 1.460; C, 1.770; H<sub>C</sub>, 1.250); P, 2.330; Hp, 1.440.  $(\text{PH}_3)_2\text{Pt}(\text{CH}_3)_2$ : Outer, 7.620; Pt, 2.522; C, 1.707; H<sub>C</sub>, 1.239; P, 2.208; Hp, 1.440.  $(\text{PH}_3)_3\text{Ni}(\text{CH}_3)_2$ : Outer, 7.620; Ni, 2.440; C, 1.770; H<sub>C</sub>, 1.250; P, 2.300; Hp, 1.440.  $(\text{PH}_3)_3\text{Pd}(\text{CH}_3)_2$ , Outer, 7.872; Pd, 2.381; C, 1.784; H<sub>C</sub>, 1.249; P, 2.356; Hp, 1.443.
22. Weast, R. Editor "Handbook of Chemistry and Physics" Chemical Rubber Co., Cleveland, Ohio, 1969, p E-80 (C, H); p E-74 (Pt, Pd, Ni).
23. For transition state configurations assumed were:  $\text{Pt}(\underline{d}^{9.5})$ ;  $\text{Pd}(\underline{d}^{9.5})$ ;  $\text{Ni}(\underline{d}^{8.5}\underline{s}^{1.5})$ . The configuration used for nickel was that recommended by Schwartz (Schwartz, K. J. Phys. B. 1978, 11, 1339-1351).
24. Bartolotti, L. J.; Gadre, S. R.; Parr, R. G. J. Am. Chem. Soc. 1980, 102, 2945-2948.
25. Although the charge distributions estimated in this method are not highly accurate, they seem to be in general agreement with values estimated experimentally: Chatt, J.; Leigh, G. J. Agnew. Chem. Intern. Ed. Engl. 1978, 17, 400-407.

26. Hoffmann, R. Accounts Chem. Res. 1971, 4, 1-9. Hetlbronner, E.; Bock, H., "The HMO Model and Its Application" Wiley Interscience, New York, 1976.
27. Hine, J., "Structural Effects on Equilibria in Organic Chemistry" Wiley-Interscience, New York, 1975. Lowry, T. H.; Richardson, K. S. "Mechanism and Theory in Organic Chemistry" Harper and Row, Publishers, New York, 1976. Norton (ref. 5) has discussed possible correlations between rates and exothermicities of organic reactions.
28. Cullen, W. R. Adv. Inorg. Chem. Radiochem. 1972, 15, 323-374.

### Captions

Figure 1. Eigenvalues for  $L_2PtXY$  [ $XY = HH$  (top),  $CH_3-H$  (middle),  $CH_3-CH_3$  (bottom)]. Only the orbitals of  $L_2Pt$  and  $XY$  making major contributions to the molecular orbitals of  $L_2PtXY$  are indicated. The eigenvalues for  $XY$  are those calculated at the distances assumed in the complex ( $r_{HH} = 2.80 \text{ \AA}$ ,  $r_{CH_3-CH_3} = 2.73 \text{ \AA}$ ,  $r_{CH_3-H} = 2.72 \text{ \AA}$ ). In addition, the eigenvalues for  $CH_3-CH_3$  are also calculated using the bent geometry ( $C_{2V}$  symmetry) this moiety displays in the  $L_2Pt(CH_3)_2$  complex. Calculations of the distorted  $CH_3-H$  molecule displaying both  $C_{3V}$  and  $C_S$  symmetries revealed insignificant differences. The figure displays the eigenvalues obtained from the  $CH_3-H$  fragment having  $C_{3V}$  symmetry.)  $L = PH_3$  in each case.

Figure 2. Orbitals important to bonding in  $L_2PtH_2$ . The first column represents the simplified interpretation of the bonding in the orbital. The representation is: ——— strongly bonding; ——— weakly bonding; ~~~~ strongly antibonding. Thus, for example, the  $2b_2$  orbital has strong Pt-H bonding character and weak Pt-P bonding. The two hydrogens (and the two phosphorus atoms) are weakly antibonding with respect to one another. No line between nearest neighbor atoms (as between Pt and P in the  $4a_1$  orbital) indicates a weak or non-bonding interaction. If a center is omitted from the diagram, the charge assigned to it is considered sufficiently small that it effectively does not participate in the orbital. The second column sketches the orbital makeup in terms of atomic orbitals. The numbers represent the fractional charge (expressed as a percentage of two electrons) centered on each center. These charges do not add to 100 because the charge on the hydrogens in  $PH_3$  and  $CH_3$

have been omitted from the diagram. The major contributions of the orbitals on platinum are indicated on the diagram. For example, the  $2a_1$  orbital contains important contributions from  $d_{x^2-y^2}$  and  $s$  orbitals centered on platinum. The last column contains a section through the wave function. The contours are plotted at values of  $\pm 0.003$ ,  $\pm 0.009$ ,  $\pm 0.027$  and  $\pm 0.081$ , starting from the outermost.

Figure 3. Orbitals important to bonding in  $L_2Pt(H)CH_3$ . The caption for Figure 2 contains nomenclature.

Figure 4. Orbitals important to bonding in  $L_2Pt(CH_3)_2$ . The caption for Figure 2 contains nomenclature.

Figure 5. Orbitals for  $L_2Pt(0)$  for angle  $LPtL = 141^\circ$ . The caption for Figure 2 contains nomenclature.

Figure 6. Eigenvalues for  $L_2Pt(0)$  as a function of angle  $LPtL$ .

Figure 7. The response of the eigenvalues of  $L_2PtH_2$  (a) to a 10% increase in the Z-coordinate of the hydrogen atom (b). These shifts in energies were used to classify the energies as bonding (B), non-bonding (N) or antibonding (A) with respect to the Pt-H interactions.

Figure 8. Orbital correlations diagrams for decompositions of  $L_2PtXY$  to  $XY$  and  $L_2Pt$  (angle =  $102^\circ$  and  $180^\circ$ ).  $XY$  is in its ground-state geometry.

Figure 9. Eigenvalues for  $L_2M(CH_3)_2$  [M = Pt, Pd, Ni]. Only the orbitals of  $L_2M$  making major contributions to the molecular orbitals of  $L_2M(CH_3)_2$  are indicated.  $L = PH_3$  in each instance.

Figure 10. Orbitals important to bonding in  $L_2Ni(CH_3)_2$ . The caption for Figure 2 contains nomenclature.

Figure 11. Orbitals important to bonding in  $L_2Pd(CH_3)_2$ . The caption for Figure 2 contains nomenclature.

Figure 12. Orbital correlation diagrams for decomposition of  $L_2M(CH_3)_2$  to  $C_2H_6$  and  $L_2M$  (angle =  $102^\circ$ ).  $C_2H_6$  is in its ground-state geometry.

Figure 13. A schematic energy level diagram summarizing the important interactions in  $L_2MXY$ .

DATE  
ILMED

-8